

## Phenomenological theory of the metal-insulator transition

This article has been downloaded from IOPscience. Please scroll down to see the full text article.

1995 J. Phys.: Condens. Matter 7 8361

(<http://iopscience.iop.org/0953-8984/7/44/006>)

View [the table of contents for this issue](#), or go to the [journal homepage](#) for more

Download details:

IP Address: 171.66.16.151

The article was downloaded on 12/05/2010 at 22:23

Please note that [terms and conditions apply](#).

## Phenomenological theory of the metal–insulator transition

P Markoš

Institute of Physics, Slovak Academy of Sciences, Dúbravská cesta 9, 842 28 Bratislava, Slovakia

Received 16 May 1995

**Abstract.** We show that the transition of a system from the metallic to the insulating regime is accompanied by a change of the density of the Lyapunov exponents of the transfer matrix of the system. This enables us to construct the distribution of the Lyapunov exponents  $P(z)$ . It has a form  $P(z) \sim \exp(-\beta\mathcal{H}t)$ , where Hamiltonian  $\mathcal{H}$  contains the one-particle potential  $V(z)$  and the interaction term  $u(z_i, z_j)$ . In the metallic limit, this distribution has a form proposed previously by random matrix theory:  $V(z)$  is quadratic and  $u(z_i, z_j)$  converges to the interacting potential found previously by Beenakker and Rajaei. Close to the critical point of the metal–insulator transition, both  $V(z)$  and  $u(z_i, z_j)$  become dimension-dependent. In particular,  $V(z) \sim z^d$  ( $d > 2$ ) at the critical point. We also discuss the applicability of the distribution  $P(z)$  and of the one-parameter theory of MIT to the description of the insulating regime.

### 1. Introduction

Recent theoretical [1–3] and numerical [4–7] studies indicate that a complete theory of the disorder-induced metal–insulator transition (MIT) has to deal with the statistics of the conductance  $g$  in all three regimes: metallic, critical and localized. On the other hand, the most successful theories of MIT, the one-parametrical scaling theory [8] and the finite-size scaling hypothesis (FSSH) [9], deal only with the most probable value of the conductance, and of the first Lyapunov exponent (LE), respectively, and consequently provide no information about the statistics of the conductance. Our present knowledge of the form of the distribution  $P(g)$  at the critical point is based mostly on numerical studies of the different models [6, 7, 10–12], and on analytical studies in dimensions slightly larger than 2 (the critical dimension of MIT) [2, 3]. Results of these studies are rather contradictory. Their understanding needs the construction of a general theory, which could enable us to find the form of  $P(g)$  at the critical point, and their dependence on the dimension of the system.

The conductance  $g$  of a disordered sample of the form  $L^{d-1} \times L_z$  can be expressed through the Lyapunov exponents  $z_i$  of the corresponding transfer matrix as [13]

$$g = \sum_{i=1}^N \frac{1}{1 + \lambda_i} = \sum_{i=1}^N \frac{2}{1 + \cosh z_i}. \quad (1)$$

In (1),  $N = L^{d-1}$  is the number of channels,  $\lambda_i$  are eigenvalues of the matrix

$$\Lambda = [T^\dagger T + (T^\dagger T)^{-1} - 2]/4 \quad (2)$$

$T$  is transfer matrix, and  $\exp(z_i)$  are eigenvalues of matrix  $T^\dagger T$ . Thus, complete information about the probability distribution  $P(z)$  of the Lyapunov exponents also provides a complete description of the statistics of the conductance.

For the metallic regime, the joint probability distribution  $P(z)$  of the LE of the transfer matrix has been proposed on the basis of random matrix theory [14] (RMT) [15–20]. Our aim in this paper is to propose a more general form of distribution  $P(z)$ , applicable not only to a description of the metallic regime, but also to the critical and even localized regimes.

The paper is organized as follows. In the remaining part of this section we review the basic ideas of FSSH and results for the distribution  $P(z)$  in the metallic regime. In section 2 we generalize  $P(z)$  to the critical and localized regimes: we introduce the density of LE, derive the one-particle potential  $V(z)$ , propose the more general form of the interacting potential  $u(z_i, z_j)$ , and introduce the generalized ‘temperature’  $\beta$ . In section 3 we apply  $V(z)$  to derive the spectrum of the LE in all three regimes in the Q1D limit. The form of the spectrum in the insulating regime, together with results for variations of the LE, indicate that the theory of the MIT is at least two-parametrical above the critical point. Section 4 brings the generalization of the results of sections 2 and 3 to the  $d$ -dimensional systems ( $d > 2$ ). In section 5 we analyse cubic samples. We discuss the differences in the spectrum of the LE and in the variances of the LE caused by the geometry of sample. The comparison of our results with data from numerical simulations [5–7, 28] is discussed throughout the paper. A summary of the presented results is given in section 6.

### 1.1. Finite-size scaling hypothesis

In the FSSH [9], the parameters of the MIT are calculated from the system width  $L$  and disorder  $W$  dependence of the smallest positive LE  $z_1$  of the Q1D sample  $L \times L \times L_z$ . It was supposed (and verified numerically) that the  $L$  and  $W$  dependence of the most probable value  $\bar{z}_1$  of the first LE can be expressed as

$$\bar{z}_1 = \frac{L_z}{L} f\left(\frac{L}{\xi(W)}\right). \quad (3)$$

In (3),  $\xi(W)$  is the scaling parameter [9]. It diverges in the neighbourhood of the critical point  $W = W_c$  as

$$\xi(W) \propto \begin{cases} (W - W_c)^{-\nu} & W \rightarrow W_c^+ \\ (W_c - W)^{-s} & W \rightarrow W_c^- \end{cases}. \quad (4)$$

In the limit  $x \gg 1$  (i.e. far from the critical point),  $f(x) \sim 2x$  ( $\sim 2/x$ ) for the localized (metallic) regime, respectively. At the critical point

$$\lim_{x \rightarrow 0} f(x) = \zeta_1. \quad (5)$$

Both the scaling parameter  $\xi$  and scaling function  $f(x)$  play a crucial role in the generalization of the distribution  $P(z)$  to the critical region.

### 1.2. Distribution of LE in the metallic regime

Before looking for the form of  $P(z)$  in the neighbourhood of the critical point, let us follow the development achieved in recent years in the description of the metallic regime. Pichard [16] supposed that the matrix  $\Lambda$  defined in (2) has the general properties of random

matrices. Consequently, the probability distribution of Lyapunov exponents (LE)  $z_i$  has the form

$$\mathcal{P}_N(z_1, z_2 \dots) = \exp(-\beta \mathcal{H}_N) \quad (6)$$

where  $\beta = 1, 2$  and  $4$  for orthogonal, unitary and symplectic ensembles, respectively, and  $\mathcal{H}$  is the Hamiltonian

$$\mathcal{H}_N = \sum_{i < j}^N u(z_i, z_j) + \sum_{i=1}^N [v(z_i) + V(z_i)] \quad (7)$$

with the interacting potential

$$u(z_i, z_j) = -\log |\cosh z_i - \cosh z_j| \quad (8)$$

the one particle potentials

$$v(z_i) = -\frac{1}{\beta} \log |\sinh z_i| \quad (9)$$

and  $V(z)$ . While  $v(z)$  originates from the Jacobian of the transformation from variables  $\lambda$  to  $z$   $\lambda_i = (\cosh z_i - 1)/2$ , the form of the potential  $V(z)$  has to be found from the known density  $\rho(z)$  of the LE [19, 21, 22].

In the metal,  $\rho(z)$  is constant [16]. It corresponds to the quadratic potential

$$V(z) = \frac{\kappa}{2} z^2 \quad (10)$$

and to the linear spectrum of LE,  $z_i \sim i$ . The distribution  $P(z)$  with quadratic potential (10) has been used by Muttalib [27] to study of the spectrum of the LE in the metallic limit.

The distribution (6) successfully explains the qualitative features of transport in the metallic regime [16]. Its connection to the local maximum entropy *ansatz* (LMEA) [23] has been established in [24]. Recent developments, however, show that both potentials (8) and (9) need corrections: thus, Chalker and Macedo [25] proved that distribution (6) represents only the adiabatic limit of the LMEA. Moreover, Beenakker [19] found that distribution (6) does not give the correct value for the universal conductance fluctuations (UCF) in the Q1D limit. In order to reproduce the exact results, the potentials  $u$  and  $v$  in (7) should be modified. Beenakker and Rajaei [20] found that  $u$  ( $v$ ) should be replaced by  $u_{\text{BR}}$  ( $v_{\text{BR}}$ ), respectively, where

$$u_{\text{BR}}(z_i, z_j) = -\frac{1}{2} \log |\cosh z_i - \cosh z_j| - \frac{1}{2} \log |z_i^2 - z_j^2| \quad (11)$$

and

$$v_{\text{BR}}(z_i) = -\frac{1}{2\beta} \log |z_i \sinh z_i|. \quad (12)$$

Although the relations (11) and (12) have been derived only for  $\beta = 2$ , there are indications that they also hold for  $\beta = 1, 4$  [20]. They provide the starting point of our considerations.

## 2. Generalization of the probability distribution

The success of RMT in the description of the metallic regime inspired us to look for the general distribution  $P(z)$  of the LE in the form of (6).

Besides the explanation of the statistical properties of the LE in the critical regime, the distribution  $P(z)$  has to fulfill some requirements: (i) it has to describe the transition from the metallic to the localized regime when the disorder  $W$  crosses its critical value  $W_c$ ; (ii) in the metallic regime it has to reduce to the well known distribution found by Beenakker and Rajaei [20]; (iii)  $P(z)$  should depend on the dimension of the system in the neighbourhood of the critical point; and (iv) the theory has to explain the differences between the spectrum of the LE, as was found numerically for systems of different system shapes [6].

Our analysis starts from the numerical observation that the spectrum of the LE changes its form when the system undergoes the MIT [6, 32]. Although this change concerns only the start of the spectrum, we believe that it represents the crucial feature of the MIT.

Let us note here that the number of channels that are important for transport is proportional to  $L \ll N$  in the metallic limit, and is  $\ll L$  at the critical point. Therefore, it is enough to consider only the  $\mathcal{N}$  smallest LE for our purposes. Although  $\mathcal{N} \ll N$ , we suppose that  $\mathcal{N}$  is infinite in the limit of infinite volume of the considered sample.

### 2.1. Density of Lyapunov exponents

On the basis of results of numerical simulations we postulate that the MIT is accompanied in 3D systems by a change of the  $z$  dependence of the density  $\rho(z)$  of the Lyapunov exponents from the constant (in metal) to the linear (at the critical point):

$$\rho(z) = 2a_3 \times \begin{cases} z + 2L_z/\xi & W < W_c \\ z & W = W_c \\ z - 2L_z/\xi & W > W_c \end{cases} \quad d = 3 \quad (13)$$

In (13),  $a_3 = \frac{1}{2}(1/\xi_1^3)(2L/L_z)^2$  and  $\xi_1$  is a universal constant, defined in (5). It depends only on the dimension and symmetry of the problem.

As is mentioned above, relation (13) concerns only the start of the spectrum. The remaining part of spectrum is linear in all three regimes. It contains only LE that are  $\gg 1$ . The role of these LE in transport is negligible so that they can be integrated out in (6).

Relation (13) underlines the role of the scaling parameter  $\xi(W)$ : it determines not only the  $L$  and  $W$  dependence of the first LE, but also the spectrum of the LE. Owing to (4), relation (13) assures the *continuous* change of  $\rho(z)$  from a constant in the metal to the linear  $z$  dependence at the critical point. In the metallic regime,  $z_i \sim 2i \times \xi L_z/L^2 \ll 2L_z/\xi$ , and so  $\rho(z)$  is almost constant, as it should be. Above the critical point, a gap is opened,  $z > 2L_z/\xi$ .

As is seen in figure 1, relation (13) is valid only in the limit of large system size, or for Q1D systems with  $L_z/L \gg 1$ . For small samples, deviations from (13) arise. It particularly concerns the localized regime, where, due to the fluctuations of the smallest LE,  $\rho(z)$  has an exponentially small tail in the gap  $z < 2L_z/\xi$ . The non-zero values of  $\rho(z)$  in the gap are responsible for the anomalous properties of the conductance in the localized regime [6]. Nevertheless, in the limit  $L \gg \xi(W)$  (strong localization), this tail does not influence our present considerations.

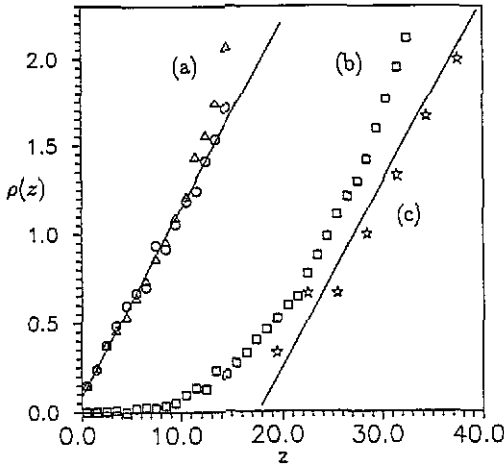


**Figure 1.** (a) Density of the LE  $\rho$  at the critical point (cubic samples). Linear fits give  $\rho \approx 0.106z + 0.086$  ( $L = 12$ ) and  $\rho \approx 0.126z - 0.0075$  ( $L = 8$ ). (b)  $\rho$  for cubes  $12^3$  and  $W = 32$ . Large fluctuations of  $\rho$  in the region of the gap represent the size effects. (c)  $\rho$  for the Q1D system  $W = 32$ ,  $L = 16$ ,  $L_z/L = 126$ . The full line is the linear fit  $\rho \approx 0.1045 \times (z - 17.65)$ . Note the constant  $2a_3 \approx 0.10$  in (13).

2.2. One-particle potential

The connection between the potential  $V(z)$  and the density  $\rho(z)$  has been established by many authors [19, 21, 22]. Here, we follow Muttalib's method [27] based on a calculation of the most probable values  $\bar{z}_i$  of the LE. The last are given as a solution of the system of equations

$$\left. \frac{\partial \mathcal{H}}{\partial z_i} \right|_{z_i = \bar{z}_i} = 0. \tag{14}$$

System (14) simplifies in the Q1D limit  $L_z \gg L$  when all  $z_i \gg 1$ . Consequently, the interacting potential  $u_g(z_i, z_j)$  reduces to  $\frac{1}{2} \log |\cosh z_i - \cosh z_j|$  and its derivative is  $\frac{1}{2}(i - 1)$ . Using the relation

$$i - 1 = \int_{\bar{z}_1}^{\bar{z}_i} \rho(z) dz \tag{15}$$

which is valid in the Q1D limit, we obtain the relation between  $\rho(z)$  and  $V(z)$ :

$$\left. \frac{\partial V(z)}{\partial z} \right|_{z = \bar{z}_i} = \frac{1}{2} \int_{\bar{z}_1}^{\bar{z}_i} \rho(z) dz + \frac{1}{2\beta}. \tag{16}$$

Relation (16) represents the special limiting case of the more general relation between  $\rho(\lambda)$  and  $V(\lambda)$ , as was derived previously [19]. After integration of (16) we get the explicit form of the potential

$$V(z) = \frac{1}{2} a_3 \left[ \frac{1}{3} (z \pm 2L_z/\xi)^3 - (\bar{z}_1 \pm 2L_z/\xi)^2 z \right] + \frac{z}{2\beta} + \text{constant} \quad d = 3. \tag{17}$$

The '+' and '-' signs correspond to the metallic and localized regime respectively, and the constant term assures that  $V(\bar{z}_1) = 0$ , as follows from (16).

### 2.3. Interacting potential

In the derivation of the one-particle potential we have assumed that the interacting potential  $u(z_i, z_j)$  is of the form (11). However, as will be discussed later, a description of the cubic systems in the critical regime requires the generalization of the interacting potential. Namely, it becomes clear that the second term in (11) should also reflect the changes of the density  $\rho(z)$  close to the critical point. As this term is negligibly small for  $z \rightarrow \infty$ , it plays no role in the Q1D limit. However, the studies of the spectrum of the cubic samples requires a knowledge of the whole potential  $u$ . We propose it to be

$$u_R(z_i, z_j) = -\frac{1}{2} \log |\cosh z_i - \cosh z_j| - \frac{1}{2} \log |V(z_i) - V(z_j)|. \quad (18)$$

A motivation for acceptance of (18) has been found in the original paper [20], where  $u_{BR}$  was derived analytically. Here, the quadratic terms  $z^2$  in the potential  $V(z)$  and in the interacting potential appear simultaneously (see equation (3.2) of [20]). We can rewrite  $u_{BR}(z_i, z_j)$  in the form of (18) when  $V(z) \propto z^2$ . It is therefore natural to assume the strong correlation between the form of the potential  $V(z)$  and of  $u(z_i, z_j)$ . We conjectured that this correlation also survives outside the metallic limit and in the general  $d$ -dimensional case.

### 2.4. The temperature $\beta$

As will be shown below, the Hamiltonian  $\mathcal{H}$  becomes size-independent for cubic samples above the critical point. To assure the true statistics of the LE, namely the system-size dependence of the variances of the LE, we have to redefine  $\beta$  in the localized limit. We propose its generalization to the form

$$\beta \rightarrow \bar{\beta} = \begin{cases} \beta & W \leq W_c \\ \beta \times \frac{z_1(W = W_c)}{z_1} & W \geq W_c. \end{cases} \quad (19)$$

In what follows we apply the distribution  $P(z)$  (6) with the generalized Hamiltonian  $\mathcal{H}$  and  $\beta$  to Q1D and 3D systems and compare the predictions of the theory with results of the numerical studies of the Anderson model.

## 3. Spectrum of quasi-one-dimensional systems

In this section we use the distribution  $P(z)$  with the one-particle potential  $V(z)$  given by (17) in the derivation of the spectra of the LE in all three regimes. As  $L_z \gg L$ , the interacting potential  $u(z_i, z_j)$  reduces to  $\frac{1}{2} \log |\cosh z_i - \cosh z_j|$ .

### 3.1. Metal

In the metallic limit,  $z \ll 2L_z/\xi$  for  $W \ll W_c$  and  $f(x) \sim 2/x$ . Taking

$$f(x) = \frac{\xi_1^3}{8\beta} x \quad x \rightarrow 0 \quad W \ll W_c \quad (20)$$

the potential  $V(z)$  reduces to the quadratic form

$$V(z) = \frac{1}{2} \kappa z^2 \quad \kappa = \frac{4}{\xi_1^3} \left(\frac{L}{\xi}\right)^2 \left(\frac{\xi}{L_z}\right) \quad W \ll W_c \quad (21)$$

and the spectrum of the LE becomes linear:

$$z_i = \frac{2L_z \xi}{L^2} \frac{\xi_1^3}{16} \left(i - 1 + \frac{1}{\beta}\right) \quad (22)$$

which reproduces correctly the numerical data [9]. Formula (20) also provides us with the coefficient of proportionality  $c$  for the scaling function  $f(x)$ .

### 3.2. Critical point

At the critical point,  $\bar{z}_1 = (L_z/L)\zeta_1$  and  $\xi \rightarrow \infty$ . The potential has a simple form:

$$V(z) = \frac{1}{6}a_3z^3 - \left(\frac{1}{\zeta_1} - \frac{1}{2\beta}\right)z \quad W = W_c \quad (23)$$

and the spectrum of the LE is

$$\bar{z}_i = \frac{L_z}{L}\zeta_1\sqrt{1 + \frac{1}{2}\zeta_1(i-1)}. \quad (24)$$

This agrees very well with the numerical data: in the Q1D Anderson model with width  $L = 18$  we have found that  $\bar{z}_i$  follow the relation  $\bar{z}_i^2 = \bar{z}_1^2[1 + a(i-1)]$  with  $a = 1.685 \approx \zeta_1/2$ .

### 3.3. Insulator

In the insulating regime we have

$$V(z) = \frac{a_3}{2}\left[\frac{1}{3}(z - 2L_z/\xi)^3 - \left(\frac{L_z}{L}\delta_1\right)^2 z\right] + \frac{z}{2\beta} \quad W > W_c \quad (25)$$

where  $\delta_1$  is given by the relation

$$\bar{z}_1 = \frac{L_z}{L}\left(\frac{2L}{\xi} + \delta_1\right). \quad (26)$$

Owing to (3)

$$\delta_1 = [f(x) - 2x] \sim O(1) \quad \text{for } x \gg 1. \quad (27)$$

For 1D systems, relation (26) has also been derived analytically [31]. The parameter  $\delta_1$  depends weakly on the strength of the disorder. As it enters the theory via the lower bound of the integration in (16), it has to be estimated numerically. Owing to (26),  $\delta_1(W = W_c) = \zeta_1$ . Above the critical point,  $\delta_1$  grows slowly with disorder and achieves its limiting value  $\delta_1 \approx 3.9$  for  $W \geq 20$ .

From potential (25) we found the spectrum of the LE:

$$z_i = \frac{2L_z}{\xi} + \frac{L_z}{L}\delta_i \quad (28)$$

where

$$\delta_i = \sqrt{\frac{1}{2}\zeta_1^3(i-1) + \delta_1^2}. \quad (29)$$

We tested relations (28) and (29) numerically (see figure 2) and found that  $z_i = \alpha_i L + \delta_i$  with slope  $\alpha_i$  almost independent of the index  $i$ , in agreement with (28). Both the small differences between  $\alpha_i$  and about 10% deviations of the numerical data for  $\delta_i$  are probably caused by the finite-size effect: the number of LE which follow (28), (29) is small for the finite system width,  $L$ , achievable by computer.

Formula (28) explains both the  $W$  and  $L$  independence of the differences [28]:

$$\frac{L}{L_z}(z_i - z_1) \propto O(1) \quad \frac{L}{\xi} \gg 1. \quad (30)$$



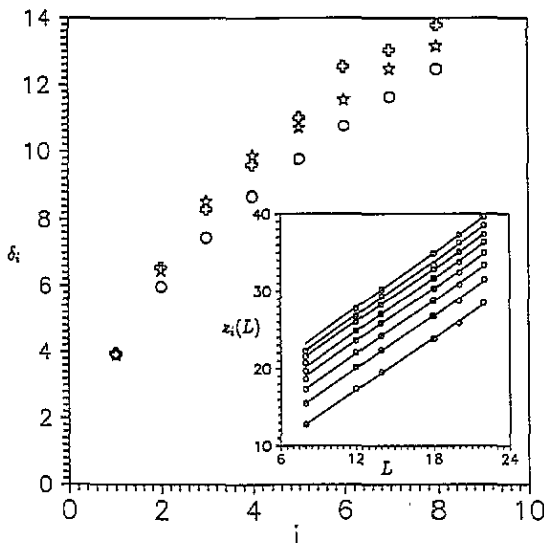


Figure 2.  $\delta_i$  against  $i$  for the Q1D system  $W = 25$  (stars) and  $W = 32$  (crosses) compared with the prediction of the formula (29) for  $\delta_1 = 3.9$  (circles). Insert: the  $L$  dependence of the eight smallest LE ( $W = 32$ ). Full lines are linear fits  $z_i = \alpha L + \delta_i$  with slopes between 1.108 ( $z_1$ ) and 1.17 ( $z_8$ ). Only data for  $L \geq 14$  have been used for the calculation of parameters  $\alpha_i, \delta_i$ .

#### 4. Fluctuations of the LE

Thanks to the statistical independence of  $z_i$  in the Q1D limit, we can estimate the variances  $\text{var } z_i = \langle z_i^2 \rangle - \langle z_i \rangle^2$  of the LE as

$$\frac{1}{\text{var } z_i} = \beta \left. \frac{\partial^2 \mathcal{H}}{\partial z_i^2} \right|_{z_i = \bar{z}_i} \tag{31}$$

It gives

$$\text{var } z_i \approx \begin{cases} (\beta \kappa)^{-1} = 2z_1 & W \ll W_c \\ (\beta a_3 \bar{z}_i)^{-1} & W = W_c \\ \frac{\zeta_1^2 z_1}{2\beta \delta_i} & W \gg W_c. \end{cases} \tag{32}$$

A numerical test of the relation (31) shows good agreement in the metallic and the critical regimes. In the insulating regime, agreement with numerical data is only qualitative (figure 3). It could be caused by inaccuracy of the numerical estimation of the variances, by finite-size effects, or by oversimplification of the relation (19).

The  $\delta_1$  dependence of  $\text{var } z_1$  in the insulating regime

$$\text{var } z_1 = \zeta_1^2 / (2\beta \delta_1) \times \bar{z}_1 \tag{33}$$

underlines the role of the parameter  $\delta_1$ . We speculate that  $\delta_1$  represents the second independent parameter of the theory. This would mean that the one-parameter scaling fails above the critical point. A numerical test of such consideration is, however, very difficult. It requires an analysis of the  $\xi$  dependence of  $\delta_1$ . We leave this question open, and simply note that the failure of the one-parameter scaling, has also been observed in (numerical and analytical) studies of the statistics of the LE in 1D chains [31].

Formulae (32) have an interesting application for the numerical analysis of the MIT. They enable us to estimate the length  $L_z$  of the Q1D system which assures that the relative

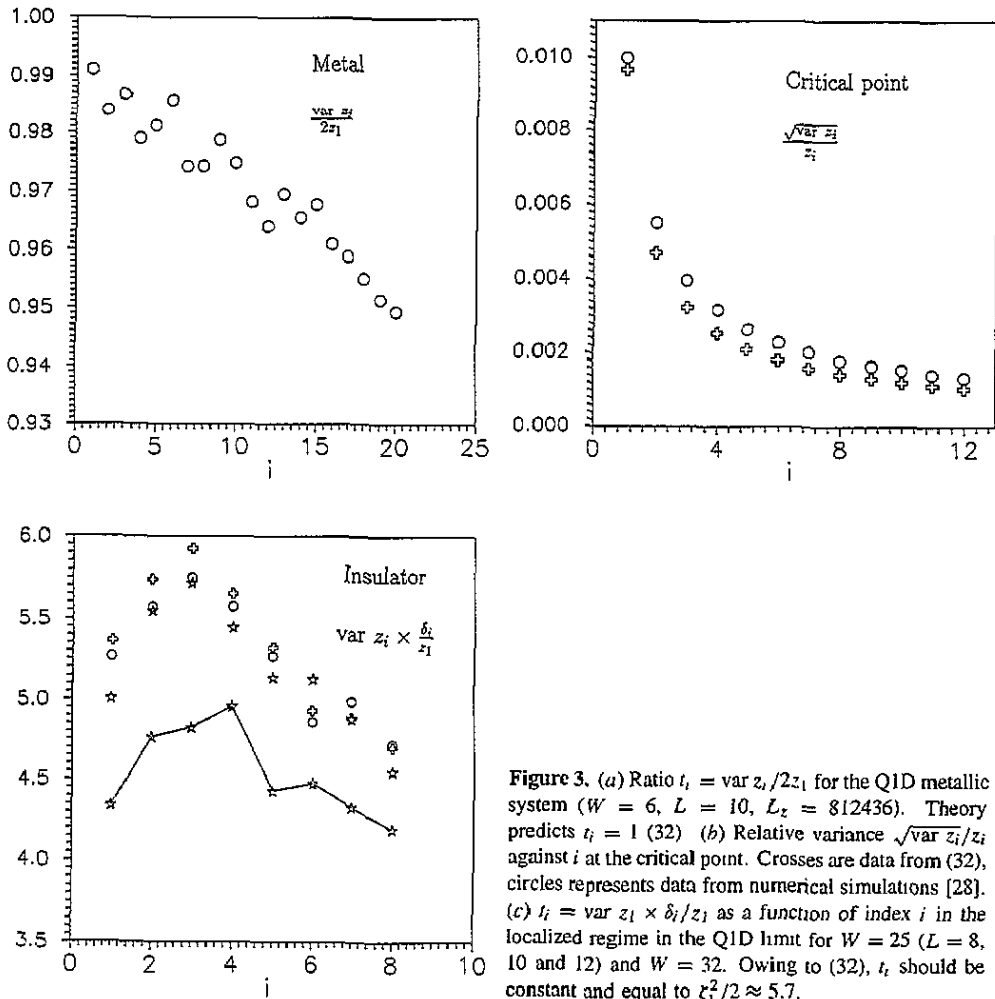


Figure 3. (a) Ratio  $t_i = \text{var } z_i / 2z_i$  for the Q1D metallic system ( $W = 6, L = 10, L_z \approx 812436$ ). Theory predicts  $t_i = 1$  (32) (b) Relative variance  $\sqrt{\text{var } z_i} / z_i$  against  $i$  at the critical point. Crosses are data from (32), circles represents data from numerical simulations [28]. (c)  $t_i = \text{var } z_i \times \delta_i / z_i$  as a function of index  $i$  in the localized regime in the Q1D limit for  $W = 25$  ( $L = 8, 10$  and  $12$ ) and  $W = 32$ . Owing to (32),  $t_i$  should be constant and equal to  $\xi_1^2 / 2 \approx 5.7$ .

variance,  $\sqrt{\text{var } z_i} / z_i$ , of the smallest LE  $z_1$  is smaller than the required accuracy  $\varepsilon$  (usually of order of 1%). We obtain

$$L_z \approx \varepsilon^{-2} \times \begin{cases} \frac{16\beta}{\xi_1^3} \frac{L^2}{\xi(W)} & W < W_c \\ \frac{1}{2\beta} L & W = W_c \\ \frac{\xi_1^2 \xi(W)}{4\delta_1 \beta} & W > W_c. \end{cases} \quad d = 3 \quad (34)$$

For simplicity, we considered the limit  $L \gg \xi(W)$  outside of the critical point in (34).

Owing to (34), the calculation of the first LE at the critical point with accuracy 1% requires consideration of the Q1D system of length  $L_z = 5000 \times L$ . This agrees with results of the numerical calculation [28].

### 5. Generalization to dimension $d > 2$

To study the general  $d$ -dimensional problem ( $d > 2$ ), it is natural to conjecture the following generalization of relation (13):

$$\rho(z) \propto 2a_d \times \begin{cases} (z + 2L_z/\xi)^{d-2} & W < W_c \\ z^{d-2} & W = W_c \\ (z - 2L_z/\xi)^{d-2} & W > W_c \end{cases} \quad d > 2 \quad (35)$$

with  $a_d = \frac{1}{2}(2L/L_z)^{d-1}\zeta_1^{-d}$ ;  $\zeta_1 = \zeta_1(d)$  is again a universal constant. Its  $d$  dependence has been conjectured to be [32]

$$\zeta_1(d) = \zeta_1(d=3) \times \sqrt{d-2}. \quad (36)$$

Using relation (35), the potential  $V(z)$

$$V(z) = \frac{a_d}{d-1} \left( \frac{1}{d} (z \pm 2L_z/\xi)^d - (\bar{z}_1 \pm 2L_z/\xi)^{d-1} z \right) + \frac{z}{2\beta} \quad (37)$$

and the spectrum of the LE have been found in the same way as in the previous section (in the Q1D limit). We briefly summarize the results.

In the metallic regime, one recovers the quadratic potential and the linear spectrum of the LE:

$$z_i = \frac{2L_z}{\xi} \left( \frac{\xi}{L} \right)^{d-1} \times 4 \times \left( \frac{\zeta_1}{4} \right)^d \times \left( i - 1 + \frac{1}{\beta} \right). \quad (38)$$

At the critical point, we have

$$z_i = z_i \times \left( 1 + \frac{d-1}{2^{d-1}} \zeta_1 (i-1) \right)^{1/(d-1)} \quad (39)$$

and the potential is

$$V(z) = \frac{a_d}{d-1} \left( \frac{z^d}{d} - \bar{z}_1^{d-1} z \right) + \frac{z}{2\beta}. \quad (40)$$

For  $d = 4$  we found numerically the spectrum  $\bar{z}_i^3 \approx \bar{z}_1^3 [1 + 1.86(i-1)]$  with  $\zeta_1 \approx 4.88$  [32]. It agrees very well with (36), (39).

Similarly, the spectrum in the localized limit is

$$\bar{z}_i = \frac{2L_z}{\xi} + \frac{2L_z}{L} \left( \frac{d-1}{2^{d-1}} \zeta_1^d (i-1) + (\delta_1/2)^{d-1} \right)^{1/(d-1)} \quad (41)$$

which is also in coincidence with the results of the numerical simulations presented in [32].

### 6. Cubic samples

In this section we find the spectra and the variances of the LE of cubic samples in all three regimes. We will explain the differences between the spectrum of Q1D and cubic samples, discussed in [6].

When comparing data for Q1D and 3D samples, we have to take into account that the first LE is not self-averaged for  $W \leq W_c$  [6]. Therefore, the difference between the most probable value  $\bar{z}$  and the mean value  $\langle z \rangle$  is not negligible. As the distribution  $P(z_1)$  is very close to the Wigner surmise in the metallic and the critical regime [6],  $\bar{z}_1$  is related with  $\langle z_1 \rangle$  through the relation

$$\bar{z}_1 \approx 0.7978 \langle z_1 \rangle \quad \beta = 1. \tag{42}$$

We suppose that the form of the potential  $V(z)$  for the cubic systems ( $L = L_z$ ) remains the same as was found in the Q1D limit. Although we cannot exclude the presence of terms  $\sim L/L_z$  in  $V(z)$  (such terms are not observable in our analysis in section 4), they have not been found in the metallic regime [16, 20, 27] and there is no reason to expect their appearance in the critical regime. The exponential ‘tail’ in the density of the LE  $\rho(z)$ , discussed in section 2.1, causes only corrections of order of  $\exp(-L/\xi)$  and can also be neglected.

#### 6.1. Metal

In the metallic limit,  $z_i \ll 1$  for  $i \leq \mathcal{N}$ . The potential is quadratic (21), and  $u(z_i, z_j) = u_{BR}(z_i, z_j)$ . We find the most probable values of the LE in the same way as was done by Muttalib [27]: as  $z_i \leq 1$  for some first Lyapunov exponents with index  $i \leq \mathcal{N}$ , we expand the ‘Hamiltonian’ (7) into a power series in  $z_i$  for  $i < \mathcal{N}$ , obtaining (for  $\beta = 1$ )

$$\mathcal{H} = - \sum_{i < j}^{\mathcal{N}} \log |z_i^2 - z_j^2| - \frac{1}{2} \sum_i^{\mathcal{N}} \log z_i^2 + \frac{\kappa}{2} \sum_i^{\mathcal{N}} z_i^2 + \dots \tag{43}$$

Inserting (43) into (14) and solving the obtained system of equations by the Stiltjes method [14, 27] we express  $\bar{z}_i$  through zeros  $x_{\mathcal{N}}(i)$  of the Laguerre polynomial  $L_{\mathcal{N}}(x)$  as

$$\bar{z}_i \approx \sqrt{\frac{x_{\mathcal{N}}(i)}{\kappa}} \quad i < \mathcal{N}. \tag{44}$$

It confirms the linearity of the spectrum of LE for large index  $i$ . Indeed, the zeros of the Laguerre polynomial can be expressed through the zeros  $j_0(i)$  of the Bessel function  $J_0(x)$  as  $x_{\mathcal{N}}(i) \approx [4(\mathcal{N} + 1/2)]^{-1} j_0^2(i) + O(1/\mathcal{N}^2)$  ( $\mathcal{N} \gg 1$ ) [29]. In the limit  $i \gg 1$   $j_0(i) \approx \pi(i - 1/4)$ ; taking  $\mathcal{N} = L/\xi$ , we have

$$\bar{z}_i = 2 \frac{\xi}{L} \frac{\pi^2}{4} i \quad i \gg 1 \tag{45}$$

which coincides with (22) if

$$\zeta_1^3 \approx 4\pi^2. \tag{46}$$

Relation (46) gives  $\zeta_1 \approx 3.405$ , in agreement with numerical data.

Owing to (44), the spectrum of the LE is not exactly linear. In particular, it gives  $\bar{z}_2/\bar{z}_1 \approx 2.3$  instead of 2. (This explains our previous numerical results [6], where we found  $\bar{z}_2/\bar{z}_1 \approx 2.5$  for  $L = 12$  and 14.) This effect is much more pronounced in 2D symplectic systems ( $d = 2, \beta = 4$ ). Here, the above-described method now enables us to express  $\bar{z}_i$  through zeros of the Laguerre polynomial  $L_N^{(-3/4)}(x)$  and obtain  $\bar{z}_2/\bar{z}_1 \approx 4.05$  unlike  $\bar{z}_2/\bar{z}_1 = 1 + \beta = 5$ , predicted by relation (22) for Q1D geometry. We checked the last two relations numerically for the 2D Ando model [30] with disorder  $W = 2$  (critical disorder  $W_c = 5.75$ ) and found  $\bar{z}_2/\bar{z}_1 \approx 3.81$  for systems  $L \times L$  with  $L \leq 100$  [7] and  $\bar{z}_2/\bar{z}_1 \approx 4.94$  for the Q1D system  $20 \times 10^5$ .

## 6.2. Critical point

As  $\bar{z}_1, \bar{z}_2, \dots \sim O(1)$  at the critical point, the Q1D result (24) also provides us with a very good approximation of the spectrum of the LE for cubes. Nevertheless, there are small differences between the spectrum of Q1D and 3D systems [6]. The most important one concerns the value of  $\langle z_1 \rangle$ . While  $\langle z_1 \rangle = \bar{z}_1 = 3.42$  for Q1D systems,  $\langle z_1 \rangle \approx 2.7$ , and  $\bar{z}_1 \approx 2.2$  in the cubic samples. We show that this difference is determined by the second term of the interacting potential  $u_g$ , which is not negligible for the cubic samples.

The mean value of the  $k$ th LE  $\langle z_k \rangle$  solves the system of equations

$$\frac{\partial}{\partial z_i} (\mathcal{H} - \log z_k) = 0 \quad i = 1, 2, \dots \quad (47)$$

We solved system (47) with potential  $V(z)$  given by (23) and interacting potential (18). The calculated spectra are presented in figure 4. To emphasize the necessity of generalization of the interacting potential, we also present in figure 4 the solution of (47) with interacting potential  $u_{BR}$ .

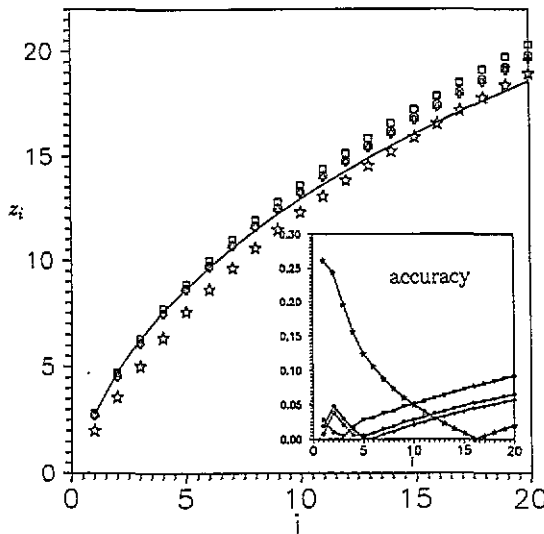


**Figure 4.** The spectrum of the LE at the critical point calculated from (47) with the interacting potential  $u_g(z_i, z_j)$  for  $N = 40$  (squares), 60 (circles) and 70 (crosses) equations. The full curve represents the result of numerical simulations [6], stars show the solution of (14) with the interacting potential  $u_{BR}$ . Insert: the relative accuracy of the calculated data for both potentials. For  $u_g$ , the accuracy is  $\leq 5\%$  for  $i \leq 12$ . For the higher LE, the agreement is worse (see text).

As is seen from figure 4, system (47) reproduces correctly the beginning of the spectra (the relative difference between the solution of (47) and the numerical data is smaller than 5% for  $i \leq 12$ , which is already comparable with the accuracy of the numerical data itself [6]). The disagreement obtained for the higher LE corresponds with an inapplicability of our formulae for the whole spectrum (see section 2).

### 6.3. Insulator

The spectrum in the insulating regime can be studied in a similar way to that at the critical point, but instead of  $z_i$  we consider the differences  $\Delta_i = z_i - 2L/\xi(W)$ . In the limit  $L/\xi \gg 1$ , we have

$$\log |\cosh z_i - \cosh z_j| \approx 2L/\xi + \log \left| \sinh \left( \frac{\Delta_i - \Delta_j}{2} \right) \right| \tag{48}$$

and

$$V(z_i) - V(z_j) = \frac{1}{3\xi_1^3} (\Delta_i^3 - \Delta_j^3) \left( \frac{\delta_1^2}{\xi_1^3} - \frac{1}{2\beta} \right) (\Delta_i - \Delta_j). \tag{49}$$

System (14) reduces then to the  $L$ -independent system of (non-linear) equations for  $\Delta_i$ . Consequently,  $\Delta_i$  achieve their limiting values, which do not depend on the disorder and on the system size in the limit  $L \gg \xi$ . Due to the differences in system (14) for the Q1D and 3D systems,  $\Delta_i$  should differ from  $\delta_i$ , introduced in section 5.3. As it is rather difficult to find numerical data for  $\Delta_i$  [5] we did not try to solve system (14) numerically.

The same effect also influences the variances of the LE. The saddle-point method now gives us

$$\text{var } z_i \approx \frac{1}{\beta} (A^{-1})_{ii} \quad A_{ij} = \left. \frac{\partial^2 \mathcal{H}}{\partial z_i \partial z_j} \right|_{z_i=\bar{z}_i, z_j=\bar{z}_j}. \tag{50}$$

Unlike in the Q1D system, the matrix  $A$  is not diagonal:

$$A_{ij} = \frac{\partial^2 V(z)}{\partial z^2} \delta_{ij} - \frac{\partial^2}{\partial z_i \partial z_j} u(z_i, z_j). \tag{51}$$

The off-diagonal terms provide us with corrections of order  $O(L/L_z)$  and  $O(\exp[-L_z/L])$  to the first one, as can be seen from equations (18), (48) and (49). They are negligible in Q1D, but not in the 3D case. This fact probably explains the geometry dependence of the variance of the logarithm of the conductance  $\log g$  in the localized regime:  $\text{var } \log g = c \langle \log g \rangle$  with  $c \approx 1$  for cubes, and  $c \approx 1.29$  for the Q1D system ( $W = 25$ ). This effect is even more pronounced in 2D systems [16].

## 7. Conclusion

We found that the density of Lyapunov exponents  $\rho(z)$  changes its form when the system undergoes a metal–insulator transition. This enables us to generalize the distribution  $P(z)$  of the Lyapunov exponents, proposed on the basis of random matrix theory, to the description of the metal–insulator transition in disordered systems. The distribution  $P(z)$  proposed previously for the metallic regime has been generalized in three points. (i) Unlike in the metallic regime, the one-particle potential  $V(z)$  becomes dimension-dependent. (ii) The interacting potential  $u_{BR}(z_i, z_j)$  derived by Beenakker and Rajaei should be generalized (18). (iii) To describe the statistics of the LE in the localized regime, we generalized the probability distribution  $P(z)$  by introducing the  $L$ -dependent ‘temperature’  $\beta$  (19).

We applied the distribution  $P(z)$  to Q1D and 3D samples and found that the predictions of the model agree very well with results of numerical simulations, particularly at the critical point and in the metallic limit. Disagreements, found in the localized regime, are probably caused by finite-size effects (numerical data have been collected for too small systems). Using the distribution  $P(z)$ , we recovered the spectrum of the LE in all three regimes in the Q1D limit, and explained the dependence of the spectrum of the LE on the geometry of the sample, discussed in [6].

The presented construction of  $P(z)$  differs from that chosen by Chen and co-workers [33], who estimated the form of the one-particle potential  $V(z)$  in the localized regime from the analogy with the distribution  $P_1(z)$  of the LE of the one-dimensional system. In our opinion, however, this correspondence is much more difficult to establish. Numerical data [5] show that the analogy between the 1D and higher-dimensional systems lies in the similar form of the distribution  $P_1(z)$  and of the distribution  $P(z_1)$  of the first LE of the higher-dimensional systems. This last is given by  $P(z_1) = \int dz_2 \dots dz_N \exp(-\beta\mathcal{H})$ . Thus  $P(z_1)$  is determined not only by  $V(z)$ , but also by the interacting potential  $u$ , and differs from  $\exp[-V(z_1)]$ .

Our results underline the important role of the finite-size scaling theory of MacKinnon and Kramer [9] in the description of the MIT: in our model, the scaling parameter  $\xi(W)$  determines not only the disorder dependence of the smallest LE  $z_1$ , but rather the whole distribution  $P(z)$  of Lyapunov exponents. On the other hand, in the localized regime we found that both the spectrum and the variance  $\text{var } z_1$  of the first LE (and so also of the conductance), depend on two parameters:  $\xi$  and  $\delta_1$ . This could explain the failure of the one-parameter scaling discussed previously [31]. As our generalization of the 'temperature'  $\beta$  is not unambiguous, we cannot discuss this problem in detail within the framework of the present paper.

The generalization of  $P(z)$  to any dimension  $d > 2$  is straightforward. We presented the formulae for the spectrum of the 4D Anderson model, which has been confirmed by numerical simulations.

The generalization of the formulae (35), (37) to the 2D systems is of particular interest. In the first approximation, the statistics of the LE in the metallic limit and at the critical point could be described starting with the quadratic potential  $V(z)$ , as was discussed in section 6.1 for the metallic limit. However, we have not succeeded in finding a consistent expression for the density of the LE in 2D. The existence of the  $\log L$  corrections to the conductance [34] indicates that both  $\rho(z)$  and the potential contain  $\log$ -dependent terms. We believe that the generalization of the present treatment will also explain the differences in the statistics of  $\log g$  in the 2D system [16].

The distribution  $P(z)$  has been obtained phenomenologically, using the numerical data for the spectrum of Lyapunov exponents. It explains very well the spectrum and the statistics of the LE. It is worth mentioning that no additional constants are necessary to fit the numerical data for  $d > 2$ . We conclude, therefore, that  $P(z)$  could be used as at least the first approximation of the exact formulae. It could be confirmed by numerical studies of other models that exhibit a MIT (the random wire model [4], for instance), or by microscopic theory, starting 'from first principles' as in [23, 25, 35, 36]. We believe that such a theory exists, and that further studies in this field will confirm our conjectures.

## Acknowledgments

I thank M Henneke for providing me with his numerical data on the quasi-one-dimensional Anderson model [28], and C W J Beenakker who brought my attention to his papers [20]

about the interacting potential. This work was supported by the Slovak Grant Agency, grant no 2/999142/93. Part of this work was performed during my participation at the NATO-ICTP Workshop on Submicron Quantum Dynamics (ICTP Trieste, June 1994). I thank ICTP for the hospitality, and the Slovak Literature Foundation for covering my travel expenses.

## References

- [1] Shapiro B 1987 *Phil. Mag.* B **56** 1032; 1990 *Phys. Rev. Lett.* **65** 1510
- [2] Altshuler B L, Kravtsov V E and Lerner I V 1986 *Sov. Phys.-JETP* **64** 1352; 1986 *JETP Lett.* **43** 441
- [3] Cohen A and Shapiro B 1992 *Int. J. Mod. Phys.* **6** 1243
- [4] Avishai Y, Pichard J-L and Muttalib K A 1993 *J. Phys. I France* **3** 2343
- [5] Markoš P and Kramer B 1993 *Ann. Phys.* **2** 339
- [6] Markoš P and Kramer B 1993 *Phil. Mag.* B **68** 357
- [7] Markoš P 1994 *J. Phys. I France* **4** 551
- [8] Abrahams E, Anderson P W, Licciardello D C and Ramakrishnan T V 1979 *Phys. Rev. Lett.* **42** 673
- [9] MacKinnon A and Kramer B 1981 *Phys. Rev. Lett.* **47** 1546; 1983 *Z. Phys.* B **53** 1
- [10] Markoš P 1994 *Europhys. Lett.* **26** 431
- [11] Bell P M and MacKinnon A 1994 *J. Phys.: Condens. Matter* **6** 5423
- [12] Cohen A, Roth Y and Shapiro B 1988 *Phys. Rev.* B **38** 12 125
- [13] Fisher D S and Lee P A 1981 *Phys. Rev.* B **23** 6851  
Pichard J-L 1984 *Thesis* Univ. Paris Sud
- [14] Mehta M L 1991 *Random Matrices* 2nd edn (New York: Academic)
- [15] Imry Y 1986 *Europhys. Lett.* **1** 249
- [16] Pichard J-L 1991 *NATO ASI Series B* **254** (New York: Plenum) p 369
- [17] Pichard J-L, Zanon N, Imry Y and Stone A D 1990 *J. Physique* **51** 587
- [18] Zanon N and Pichard J-L 1988 *J. Physique* **49** 907
- [19] Beenakker C W J 1993 *Phys. Rev.* B **47** 15 763
- [20] Beenakker C W J and Rajaei R 1994 *Phys. Rev.* B **49** 7499
- [21] Balian R 1968 *Nuevo Cimento* **57** 183
- [22] Dyson F J 1972 *J. Math. Phys.* **13** 90
- [23] Melo P A, Pereyra P and Kumar N 1988 *Ann. Phys., NY* **181** 290
- [24] Muttalib K A, Pichard J-L and Stone A D 1987 *Phys. Rev. Lett.* **59** 2475
- [25] Chalker J T and Macedo A M S 1993 *Phys. Rev. Lett.* **71** 3693
- [26] Pichard J-L and Andre G 1986 *Europhys. Lett.* **2** 477
- [27] Muttalib K A 1990 *Phys. Rev. Lett.* **65** 745
- [28] Henneke M *private communication*
- [29] Abramowitz M and Stegun I E 1979 *Handbook of Mathematical Functions* (New York: Dover)
- [30] Ando T 1989 *Phys. Rev.* B **40** 5325
- [31] Slevin K and Pendry J B 1990 *J. Phys.: Condens. Matter* **2** 2821  
Roberts P J 1992 *J. Phys.: Condens. Matter* **4** 7795
- [32] Markoš P and Henneke M 1994 *J. Phys.: Condens. Matter* **6** L765
- [33] Chen Y, Ismail H E M and Muttalib K A 1992 *J. Phys.: Condens. Matter* **4** L417
- [34] Wegner F 1979 *Z. Phys.* B **35** 207
- [35] Dorokhov O N 1982 *Sov. Phys.-JETP Lett.* **36** 318
- [36] Melo P A and Tomsovic S 1992 *Phys. Rev.* B **46** 15963